

## CO oxidation on a Cu(100) catalyst

János Szanyi and D. Wayne Goodman<sup>1</sup>

*Department of Chemistry, Texas A&M University, College Station, TX 77843-3255, USA*

Received 2 March 1993; accepted 11 May 1993

The oxidation of carbon monoxide by molecular oxygen on a single crystal Cu(100) catalyst was studied at 458 K using reactant gas mixtures with CO/O<sub>2</sub> ratios of 2/1, 10/1 and 25/1 at a total pressure of 10 Torr. The catalytic activities were found to be strongly dependent upon the CO/O<sub>2</sub> ratio. Under stoichiometric reaction conditions (CO/O<sub>2</sub> = 2), the initial CO oxidation activity decreased sharply; with a highly reducing reaction mixture (CO/O<sub>2</sub> = 25), the initial activity gradually increased. These changes in catalytic activities with reactant gas mixture composition correlate with changes in surface composition, namely an increase in the surface oxygen coverage. Post-reaction TPD revealed the presence of a carbonate-like species which decomposed at ca. 630 K.

**Keywords:** CO oxidation; Cu(100)

### 1. Introduction

The removal of CO from exhaust gases emitted by automobiles and heavy industry is a major environmental concern. The catalytic oxidation of CO is a very efficient way to convert CO to CO<sub>2</sub>. For example, in catalytic converters, the supported noble metals Pt, Pd and Rh have been used widely and effectively to improve automotive emissions. With respect to the details of the reaction, numerous studies have been carried out on both supported [1–4] and single crystal [5–7] catalysts.

Supported CuO is known to be an effective CO oxidation catalyst [8–11]. Zeolites, ion exchanged with Cu, have been studied with respect to CO oxidation and NO decomposition [12–16]. A thorough kinetic study of CO oxidation on a reduced Al<sub>2</sub>O<sub>3</sub>-supported Cu catalyst has also been carried out [17].

With respect to single crystal studies on Cu, a series of investigations has been conducted to explore the adsorptive and catalytic properties of different faces [18–21]. The adsorption of oxygen and CO and the interaction between O(a) and CO(a) have been compared on the (100), (110) and (111) orientations of Cu.

<sup>1</sup> To whom correspondence should be addressed.

On the basis of the results for supported Cu/Al<sub>2</sub>O<sub>3</sub> and for the single crystal Cu catalysts, the following general conclusions can be drawn: (1) Oxygen adsorbs strongly on Cu and forms CuO<sub>x</sub> at temperatures > 300 K. (2) CO adsorbs weakly on Cu and the adsorption of O<sub>2</sub> inhibits CO adsorption. (3) The reaction of CO + O<sub>2</sub> on Cu catalysts follows the Langmuir–Hinshelwood mechanism, i.e., the reaction takes place on the surface between CO(a) and O(a) to produce CO<sub>2</sub>. The activation energy for this process is estimated to be 18–22 kcal/mol.

In the present study CO oxidation on a Cu(100) single crystal has been carried out using reactant gas mixtures with different CO/O<sub>2</sub> ratios. The catalytic activity and changes in the surface composition following reaction were followed using elevated pressure kinetics, Auger electron spectroscopy (AES) and temperature programmed desorption (TPD).

## 2. Experimental

The experiments were carried out in a combined elevated pressure reactor–ultra-high vacuum (UHV) surface analytical chamber which is described in detail elsewhere [22]. The UHV chamber, with a base pressure of  $<3 \times 10^{-10}$  Torr, is equipped with Auger electron spectroscopy, temperature programmed desorption, ion sputtering and gas- and metal-dosing capabilities. The crystal was heated resistively by a tantalum wire swaged into grooves located at the sample perimeter. The temperature of the crystal was monitored using a W–5% Re/W–26% Re thermocouple pressed into a small well located on the edge of the sample.

Argon ion sputtering followed by annealing to 800 K were used to clean the Cu(100) sample; cleanliness was verified by AES. Following the cleaning procedure described above, the crystal was transferred into the reaction chamber, contiguous to the surface analytic chamber, through three doubly-differentially pumped teflon sliding seals. Pressures up to 760 Torr can be maintained in the reaction chamber without any measurable pressure increase in the UHV chamber. The batch reactor (490 cm<sup>3</sup>) is connected to a gas handling system and a gas chromatograph (GC) equipped with a flame ionization detector (FID). The GC separation column is connected to a methanizer which converts the CO and CO<sub>2</sub> quantitatively to CH<sub>4</sub>.

Upon completion of a catalytic experiment the reactant–product gas mixture was evacuated through the GC sample loop emersed in a liquid nitrogen bath, a procedure that ensured the efficient trapping of all CO<sub>2</sub> produced. The CO<sub>2</sub> product was analyzed by warming the sample loop to  $T > 350$  K. This analysis method allowed the measurement of CO<sub>2</sub> with high sensitivity and accuracy. The GC calibration was periodically checked for CO<sub>2</sub> within the concentration range of interest.

Research purity (>99.999%, Matheson) gases of CO and O<sub>2</sub> were used. CO was passed through a 142 K *n*-pentane/liquid nitrogen slurry trap to remove metal

(Ni, Fe) carbonyls. Oxygen was used as received. Mixtures of CO + O<sub>2</sub> with varying ratios were prepared in a liter glass bulb and allowed to mix >12 h to ensure homogeneity.

After completion of a kinetic experiment the crystal was transferred back to the UHV chamber where the surface composition was assessed with AES and TPD.

### 3. Results and discussion

The initial activity of a Cu(100) catalyst for CO oxidation was investigated in the temperature range of 458–525 K using a CO/O<sub>2</sub> = 10 reactant gas mixture; the results are displayed in Arrhenius form in fig. 1. The rates of reaction are expressed as turnover frequencies or the number of CO<sub>2</sub> molecules produced per surface Cu atom per second. The apparent activation energy determined from the slope of the Arrhenius plot of fig. 1 was  $6.5 \pm 0.5$  kcal/mol, in good agreement with the value of  $6.9 \pm 0.4$  kcal/mol determined for the reaction of CO with O(a) on a Cu(100) single crystal [21]. On the other hand the apparent activation energy value of

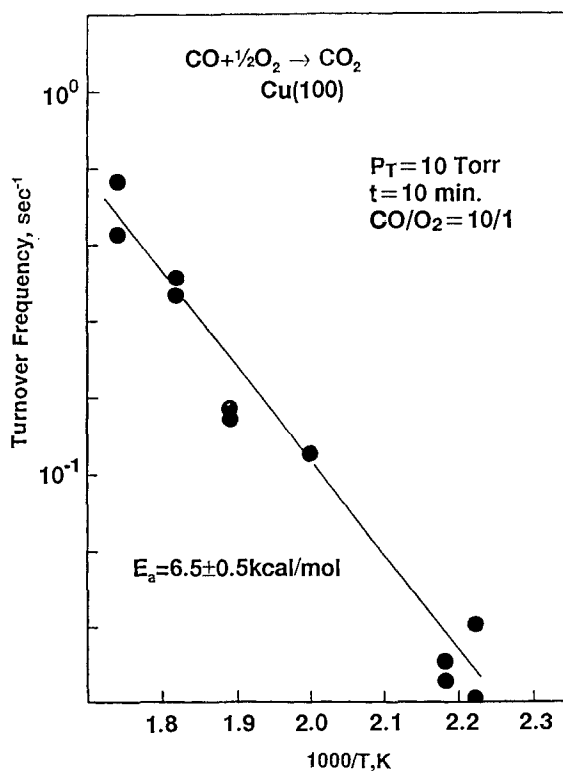


Fig. 1. Specific rate of CO<sub>2</sub> formation over Cu(100) for the CO + O<sub>2</sub> reaction. P<sub>Total</sub> = 10 Torr; CO/O<sub>2</sub> = 10/1.

$6.5 \pm 0.5$  kcal/mol is much smaller than the 17–22 kcal/mol activation energy found for a reduced Cu/Al<sub>2</sub>O<sub>3</sub> catalyst [17]. It is noteworthy that these values are apparent activation energies, not the true activation energies for the CO(a)+O(a) reaction. To obtain the true activation energy for the surface reaction, the heat of adsorption of CO on Cu(100) under the reaction conditions has to be considered. The heat of adsorption of CO on Cu(100) varies with coverage [23,24]. The CO coverage at a given temperature, in turn, is determined by the CO pressure and the CO/O<sub>2</sub> ratio.

In the present experiments a reducing (CO/O<sub>2</sub> = 10) reactant gas mixture was used to avoid oxidation of the Cu surface. Using the value of 12–13 kcal/mol from ref. [21] for the heat of adsorption of CO on Cu(100), the activation energy for CO(a)+O(a) is estimated to be  $\sim 18$  kcal/mol, close to the value reported for single crystal Cu(100) [21] and slightly lower than the value found for Cu/Al<sub>2</sub>O<sub>3</sub> [17]. The differences in activation energies, in part, can be attributed to the very different reaction conditions under which the sets of data were acquired.

The change in activity of the Cu(100) catalyst with reaction time is shown in fig. 2. The initial high activity drops sharply during the first two reaction runs and

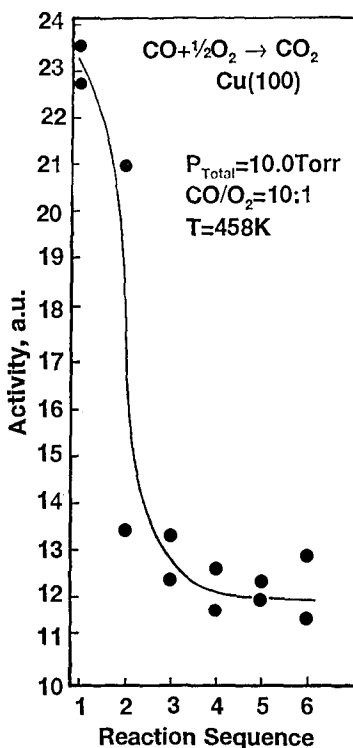


Fig. 2. Activity of Cu(100) for CO<sub>2</sub> production as a function of reaction time.  $P_{\text{Total}} = 10$  Torr;  $T = 458$  K; CO/O<sub>2</sub> = 10/1; reaction sequence = 2 min.

subsequently remains essentially constant. The steady-state activity of the catalyst is approximately one-half the initial activity. Post-reaction surface analysis indicated an increase in both the O/Cu and C/Cu Auger ratios (shown in fig. 3A) indicating the accumulation of both oxygen and carbon on the surface. Significant increases in both the oxygen and carbon levels were observed following the first reaction run. Following the second reaction run, which was carried out on this partially oxygen and carbon covered Cu surface, a further increase in both the O/Cu and C/Cu ratios was observed. On the other hand, a sharp drop in the catalytic activity was apparent on the oxidized surface. Subsequent reaction runs showed no change in either the O/Cu and C/Cu Auger ratios or the catalytic activity. These results indicate that metallic Cu has a higher catalytic activity for CO oxidation than does oxidized Cu. At the onset of reaction, both sufficient CO(a) and O(a) are present on the Cu(100) surface and the reaction proceeds rapidly. As the reaction progresses, because of the much stronger interaction between oxygen and Cu compared to CO and Cu, the Cu surface gradually becomes covered with oxygen. On this oxygen-covered Cu surface the reaction proceeds at a slower rate compared to the metallic Cu surface. As the oxygen and carbon level on the surface stabilize, the activity becomes constant and characteristic of the oxygen-covered Cu surface. The catalytic surface, however, can be considered more carbonate-like rather than oxide-like since a significant amount of carbon is present following reaction.

Following reaction the sample was heated sequentially from 450 to 800 K and AES data acquired with respect to the changes in surface oxygen and carbon coverages. As fig. 3B shows, the carbon and oxygen level decrease simultaneously in the temperature range 450–630 K. However, at 630 K significant oxygen remains

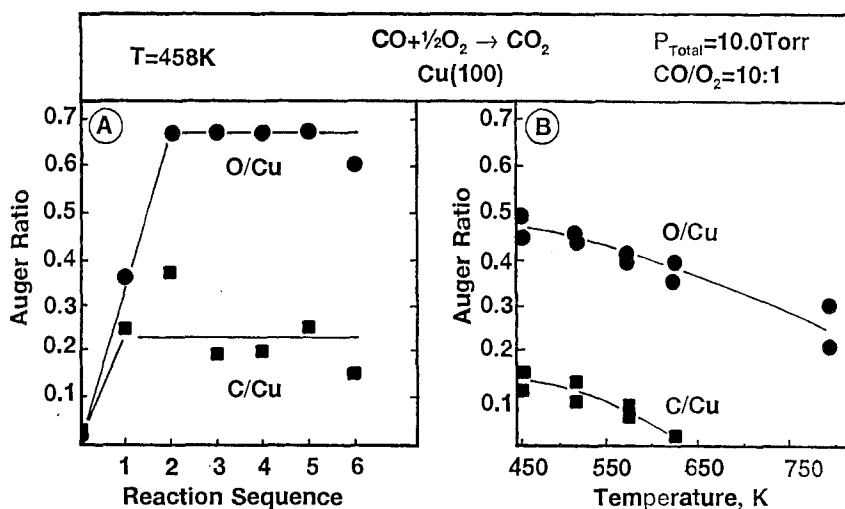


Fig. 3. (A) The build-up of oxygen and carbon on the Cu(100) surface during the CO–O<sub>2</sub> reaction as a function of reaction time.  $P_{\text{Total}} = 10\text{ Torr}$ ;  $T = 458\text{ K}$ ;  $\text{CO}/\text{O}_2 = 10/1$ ; reaction sequence = 2 min. (B) The amount of surface oxygen and carbon as a function of post-reaction annealing temperature.

after the carbon level has dropped below the AES detection limit. Flashing the sample to 800 K did not remove all of this oxygen. The residual oxygen can be attributed to an oxide layer at the Cu surface.

A similar series of experiments was carried out at 458 K on Cu(100) using a highly reducing reactant mixture ( $\text{CO}/\text{O}_2 = 25$ ). The changes in both the catalytic activity and surface composition of this mixture with reaction time are shown in fig. 4. In this series of experiments the Cu(100) sample was transferred back into the UHV chamber after every reaction and surface analysis was carried out using AES. Furthermore after every reaction, Auger and TPD were used to follow any species desorbing from the surface. Significant  $\text{CO}_2$  (mass 44) desorbed with a peak maximum temperature of about 630 K. A series of  $\text{CO}_2$  TPD spectra acquired in the temperature range of 450–850 K are displayed in fig. 5. Using this very reducing gas mixture ( $\text{CO}/\text{O}_2 = 25$ ), a different activity behavior was apparent compared

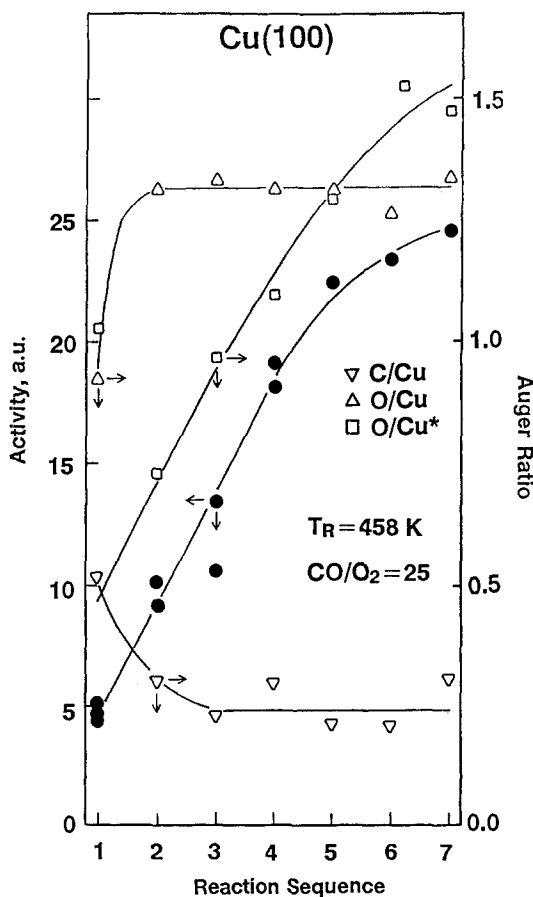


Fig. 4. The rate of  $\text{CO}_2$  production and the changes in surface composition over Cu(100) as functions of reaction time.  $P_{\text{Total}} = 10$  Torr;  $T = 458$  K;  $\text{CO}/\text{O}_2 = 25/1$ ; reaction sequence = 2 min. (\* Auger ratio measured following the post-reaction TPD experiment.)

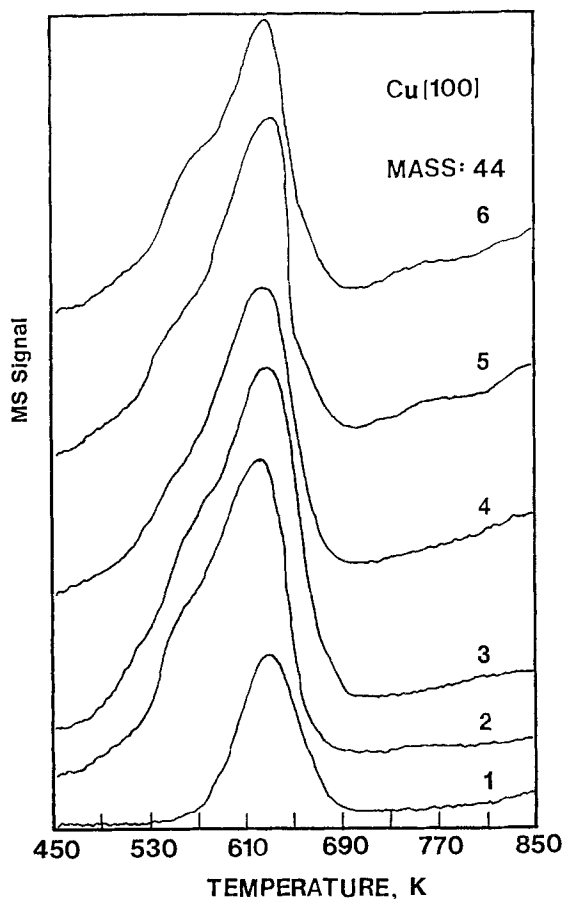


Fig. 5. Post-reaction  $\text{CO}_2$  TPD spectra. The spectra were acquired after  $\text{CO-O}_2$  reactions over  $\text{Cu(100)}$  in reaction 1 through 6 in fig. 4.

to the  $\text{CO/O}_2 = 10$  gas mixture. In this case an approximate linear increase in catalytic activity was observed during the first four reaction runs, after which the activity stabilized (fig. 4). It is noteworthy that the catalytic activity tracks exactly the O/Cu Auger ratio measured subsequent to the post-reaction TPD experiments. In addition to oxygen, post-reaction Auger analysis showed carbon on the surface. Following the first reaction the oxygen level is lower and the carbon level higher than at steady state. This is likely due to the initial large excess of CO. Under this highly reducing reaction condition, the surface is predominantly covered by CO. In subsequent reactions, however, the surface becomes increasingly covered with oxygen. After several reactions, a steady-state oxygen level is achieved; however, the large excess of surface CO quite likely prevents deep oxidation.

The formation of a carbonate-like species is apparent in the  $\text{CO}_2$  TPD. After the first reaction run, at which point the surface oxygen coverage is relatively low,

the quantity of  $\text{CO}_2$  desorbed is relatively small compared to subsequent reaction runs. Following the first reaction, the quantity of  $\text{CO}_2$  desorbed does not change appreciably, consistent with the steady-state coverages of the carbon and oxygen found in post-reaction Auger analysis. The carbon level following TPD is below the detection limit of AES; however, oxygen is still present on the surface and increases in coverage with reaction time up to the fifth reaction run. The fact that the oxygen level after the last two TPD experiments is higher than after reaction suggests that surface oxygen migrates into the Cu bulk during reaction. As the surface carbonate is removed via TPD, the subsurface oxygen diffuses to the surface. The nature of the surface carbonate species is uncertain at this point. Further XPS and HREELS studies are in progress to address this issue in detail.

The changes in catalytic activities at 458 K of the Cu(100) are summarized in fig. 6 for three gas mixtures with various  $\text{CO}/\text{O}_2$  ratios. The highest initial catalytic activity is seen for the  $\text{CO}/\text{O}_2 = 2$  mixture, which is three times higher than that for the  $\text{CO}/\text{O}_2 = 10$  and more than an order of magnitude higher than that for the

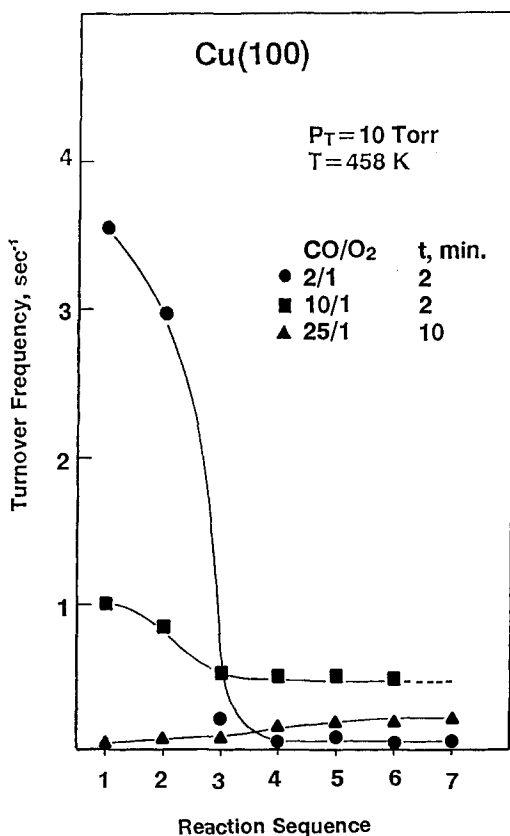


Fig. 6. Comparison of specific  $\text{CO}_2$  formation rates over Cu(100) for gas mixtures with different  $\text{CO}/\text{O}_2$  ratios as a function of reaction time.  $P_{\text{Total}} = 10 \text{ Torr}$ ;  $T = 458 \text{ K}$ .



$\text{CO}/\text{O}_2 = 25$ . However, the activity of the Cu(100) with a less reducing environment decreases very sharply. Following the third reaction run at  $\text{CO}/\text{O}_2 = 2$ , the activity is lower than that for  $\text{CO}/\text{O}_2 = 10$ . After the fourth reaction, the activity falls below the activity measured for  $\text{CO}/\text{O}_2 = 25$ . The Cu surface is significantly oxidized in the  $\text{CO}/\text{O}_2 = 2$  reactant gas mixture and, accordingly, the activity drops. The activity plots for  $\text{CO}/\text{O}_2 = 10$  and  $\text{CO}/\text{O}_2 = 25$  are obtained from fig. 2 and fig. 4, respectively.

In summary, our data on CO oxidation on a Cu(100) catalyst show that the presence of a certain level of surface oxygen is advantageous; however, under stoichiometric conditions an oxide layer forms and significantly reduces the catalytic activity compared to metallic Cu. In addition to the oxide layer, a carbonate-like species is also formed. The activation energy obtained for the  $\text{CO(a)} + \text{O(a)}$  reaction with the  $\text{CO}/\text{O}_2 = 10$  gas mixture at an elevated pressure is comparable with published data for Cu(100) under UHV conditions and supported Cu/ $\text{Al}_2\text{O}_3$  catalysts under atmospheric conditions.

## Acknowledgement

We acknowledge with pleasure the support of this work by the Department of Energy, Office of Basic Sciences, Division of Chemical Sciences and the Robert A. Welch Foundation.

## References

- [1] C.T. Campbell and J.M. White, *J. Catal.* 54 (1978) 289.
- [2] Y. Kim, S.-K. Shi and J.M. White, *J. Catal.* 61 (1980) 374.
- [3] S.H. Oh and J.E. Carpenter, *J. Catal.* 80 (1983) 472.
- [4] S.H. Oh and C.C. Eickel, *J. Catal.* 128 (1991) 526.
- [5] T. Engel and G. Ertl, *Adv. Catal.* 28 (1979) 1.
- [6] P.J. Berlowitz, C.H.F. Peden and D.W. Goodman, *J. Phys. Chem.* 92 (1988) 5213.
- [7] C.H.F. Peden, D.W. Goodman, D.S. Blair, P.J. Berlowitz, G.B. Fisher and S.H. Oh, *J. Phys. Chem.* 92 (1988) 1563.
- [8] A.V. Vorontsov, L.A. Kasatkina, A.P. Dzyzyak and S.V. Tikhonova, *Kinet. Katal.* 20 (1979) 1194.
- [9] A.V. Vorontsov and L.A. Kasatkina, *Kinet. Katal.* 21 (1980) 1494.
- [10] T.-J. Huang, T.-C. Yu and S.-H. Chang, *Appl. Catal.* 52 (1989) 157.
- [11] E.D. Pierron, J.A. Rashkin and J.F. Roth, *J. Catal.* 9 (1967) 38.
- [12] J.O. Petunchi and W.K. Hall, *J. Catal.* 80 (1983) 403.
- [13] E.E. Miro, D.R. Ardiles, E.A. Lombardo and J.O. Petunchi, *J. Catal.* 97 (1986) 43.
- [14] E.E. Miro, E.A. Lombardo and J.O. Petunchi, *J. Catal.* 104 (1986) 176.
- [15] Y. Li and W.K. Hall, *J. Phys. Chem.* 94 (1990) 6145.
- [16] H. Matsumoto and S. Tanabe, *J. Phys. Chem.* 94 (1990) 4207.
- [17] K.J. Choi and M.A. Vannice, *J. Catal.* 131 (1991) 22.
- [18] F.H.P.M. Habranek and G.A. Bootsma, *Surf. Sci.* 87 (1979) 333.

- [19] F.H.P.M. Habranek and G.A. Bootsma, *Surf. Sci.* 88 (1979) 285.
- [20] F.H.P.M. Habranek, E.P. Kieffer and G.A. Bootsma, *Surf. Sci.* 83 (1979) 45.
- [21] F.H.P.M. Habranek, C.M.A.M. Mesters and G.A. Bootsma, *Surf. Sci.* 97 (1980) 264.
- [22] J. Szanyi and D.W. Goodman, *Rev. Sci. Instr.*, in press.
- [23] J.C. Tracy, *J. Chem. Phys.* 56 (1970) 2798.
- [24] C.M. Truong, J.A. Rodriguez and D.W. Goodman, *Surf. Sci. Lett.* 271 (1992) L385.